

# HiSST: 4th International Conference on High-Speed Vehicle Science Technology 22 -26 September 2025, Tours, France



# **Experimental Investigation on the Combustion Characteristics of Paraffin- based Hybrid Gas Generators**

Zezhong Wang<sup>1</sup>, Xin Lin<sup>2</sup>, Xilong Yu<sup>3</sup>

#### **Abstract**

A hybrid gas generator (HGG) with a paraffin-based fuel grain is a high-performing gas supply alternative for rocket-based ramjet applications. Aiming to provide stable and adequate fuel-rich gas, the combustion mode of HGG was explored through theoretical analysis. The end-burning coupled with swirling injection was selected to maximize the regression rate of the fuel grain while minimizing the O/F ratio and combustion temperature. Firing tests were conducted to evaluate HGG's combustion characteristics. The performance of solid fuels with different components was compared. The PE fuel grain was tested and served as the baseline. The HGG exhibited rapid ignition and pure paraffin fuel grains demonstrated a high regression rate, linearly related to oxidizer flux, proving well-suited for HGG. Adding binders and aluminum powders significantly decreased the regression rate, which also leads to a notable rise in combustion temperature. Excess aluminum drastically lowers the regression rate and sharply raises the O/F ratio.

**Keywords**: hybrid gas generator, paraffin fuel, aluminum, regression rate, combustion property

#### **Nomenclature**

a, n	=	coefficient of regression rate	$P_{c}$	=	combustion chamber pressure
ABS	=	acrylonitrile butadiene styrene	r	=	cylinder radius
С	=	carbon	r	=	regression rate
EVA	=	ethylene-vinyl acetate	SA	=	stearic acid
copoly	mer		Τ	=	temperature
$G_{ox}$	=	mass flux of the oxidizer	$\dot{V}$	=	volumetric flow rate
$\dot{m}_f$	=	mass flow rate of the fuel	$\alpha$	=	cone half-angle
$\dot{m}_{ox}$	=	mass flow rate of the oxidizer	ho	=	density
O/F	=	oxidizer-to-fuel			

### 1. Introduction

With advantages such as low cost, reusability, and variable thrust, HRE can serve not only as the primary power system for launch vehicles, boosters, and suborbital vehicles but also as a subsystem to supply gas. GG can be categorized into three types according to the state of the propellants: LGG, SGG, and HGG. Among these, LGG can regulate the flow of gas by controlling the flow rates of propellants[1], which is suitable for the operational environment of the high-speed TMV. However, complex systems and higher costs pose certain limitations. SGG are widely adopted due to their advantages such as simple structure and short response time[2]. Nevertheless, they still face unavoidable impacts in terms of specific impulse performance and safety. Hybrid gas generators, by integrating the characteristics of the above two types, offer benefits such as simple system, adjustable flow rate, and high safety[3].

HiSST-2025-0077 Paper Title

<sup>&</sup>lt;sup>1</sup> Institute of Mechanics, Chinese Academy of Sciences, Beijing, China, wangzezhong@imech.ac.cn

<sup>&</sup>lt;sup>2</sup> Institute of Mechanics, Chinese Academy of Sciences, Beijing, China, linxin\_bit@imech.ac.cn

<sup>&</sup>lt;sup>3</sup> Institute of Mechanics, Chinese Academy of Sciences, Beijing, China, xlyu@imech.ac.cn

The application of HGG also presents challenges that need to be overcome, particularly when applied to the TMR. First, the vehicle must overcome the resistance caused by high-speed motion, which requires a high thrust. The regression rate of traditional hybrid rocket propellants is relatively low[4-6]. Low regression rate[7] led to a low gas flow rate, which makes it difficult to increase thrust. Second, changes in the burning surface area of the solid fuel grain coupled with variations in regression rate due to flux adjustments can easily result O/F ratio deviations during combustion, thereby increasing the adjustment difficulty of operating conditions.[8] Extensive research has been conducted to address the above challenges, including methods such as swirling injection[9], liquifying fuels[10], and specially designed grain structures[11] to enhance regression rates. Additionally, methods like SOFT[12] and controlled oxidizer flow[13] have been employed to control O/F ratio deviations. However, these studies primarily focus on optimizing conventional hybrid rocket engines. There has been limited research targeting the specific requirements of the HGG, which demands high combustion gas quality under extremely fuel-rich conditions.

Therefore, this work focuses on the need for a stable supply of fuel-rich gas in HGG. Theoretical analysis was conducted to clarify their structural design and operational conditions. Solid fuel grains with different compositions were prepared. Coupled with a swirling injection method, the firing test was conducted to explore the combustion characteristics of the paraffin-based HGG and figure out the influence on the regression rate of paraffin-based fuel grains by fuel composition and grain structure. Simultaneously, O/F ratio deviations were monitored, and the evolution of combustion gas temperature was examined.

# 2. Theoretical analysis

#### 2.1. Combustion mode

HGG needs to maintain a relatively stable O/F ratio to minimize the residual propellants. For HGG with traditional central-port grain structures (as shown in Fig 1a), the O/F ratio can be expressed as a function:

$$\frac{o}{F} = \frac{\dot{m}_{ox}}{\dot{m}_f} = \frac{\dot{m}_{ox}}{2\pi\rho r LaG_{ox}^n} = \frac{\dot{m}_{ox}}{2\pi\rho r La\left(\frac{\dot{m}_{ox}}{\pi r^2}\right)^n} = \frac{\dot{m}_{ox}^{1-n}}{2\pi^{1-n}\rho r^{1-2n}La}$$
(1)

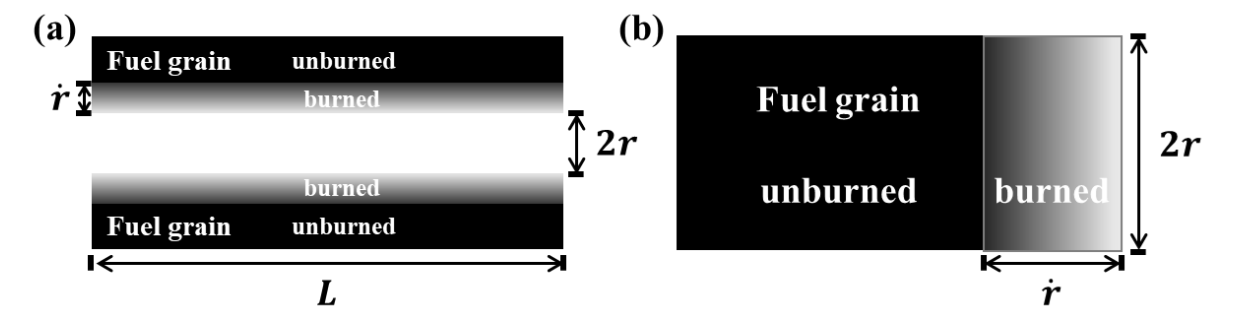


Fig 1. (a) Traditional combustion mode and (b) end-burning mode

To maintain a consistent O/F ratio regardless of the variation in  $\dot{m}_{ox}$ , the value of n must approach 1, then :

$$\frac{o}{F} = \frac{r}{2oLa} \tag{2}$$

It is still affected by the increase of r. Therefore, adopting an end-burning configuration as shown in Fig. 1b to ensure that the O/F ratio remains unaffected. Here the O/F ratio is:

$$\frac{o}{F} = \frac{\dot{m}_{ox}}{\dot{m}_f} = \frac{\dot{m}_{ox}}{\rho \pi r^2 a G_{ox}^n} = \frac{\dot{m}_{ox}}{\rho \pi r^2 a \left(\frac{\dot{m}_{ox}}{\pi r^2}\right)^n} = \frac{\dot{m}_{ox}^{1-n}}{\rho \pi^{1-n} r^{2-2n} a}$$
(3)

There is the same necessary for n to approach 1, then:

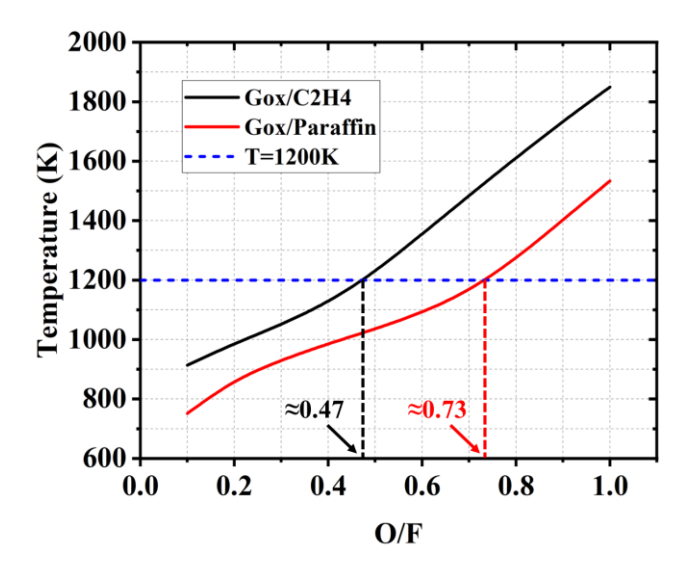
$$\frac{o}{F} = \frac{m_{ox}}{m_f} = \frac{1}{\rho a} \tag{4}$$

The O/F ratio only depends on  $\rho$  and  $\alpha$ , However, this places extremely high requirements on the

combustion performance of solid fuel.

# 2.2. Working conditions

The initial working conditions were analyzed with a gas temperature of 1200K, which corresponds to the common GG gas temperature and the Inconel 718 alloy limit operating temperature. Figure 2 shows the variation of combustion temperatures for different fuels with respect to the O/F ratio. For low-regression-rate fuels like polyethylene (PE), the target combustion temperature is achieved when the O/F ratio approaches 0.47. It is difficult to realize a linear relationship between the regression rate of the fuel grain and the oxidizer flux, making it difficult to avoid deviations in the O/F ratio.



For paraffin fuels, the combustion temperature reaches the target value when the O/F ratio approaches 0.73. The higher O/F ratio compared to that of PE fuel simplifies combustion organization and reduces the design complexity for HGG system. Paraffin fuel with an inherently high regression rate has the potential to achieve a linear relationship between the  $\dot{r}$  and  $G_{ox}$ . Meantime, it should not be overlooked that paraffin fuel suffers from inherent structural weaknesses that pose operational risks (such as layering, cracking, softening, or even collapse). It is necessary to synergistically enhance the practical performance, including both mechanical and combustion properties.

### 3. Experimental setup

#### 3.1. Hybrid gas generator system

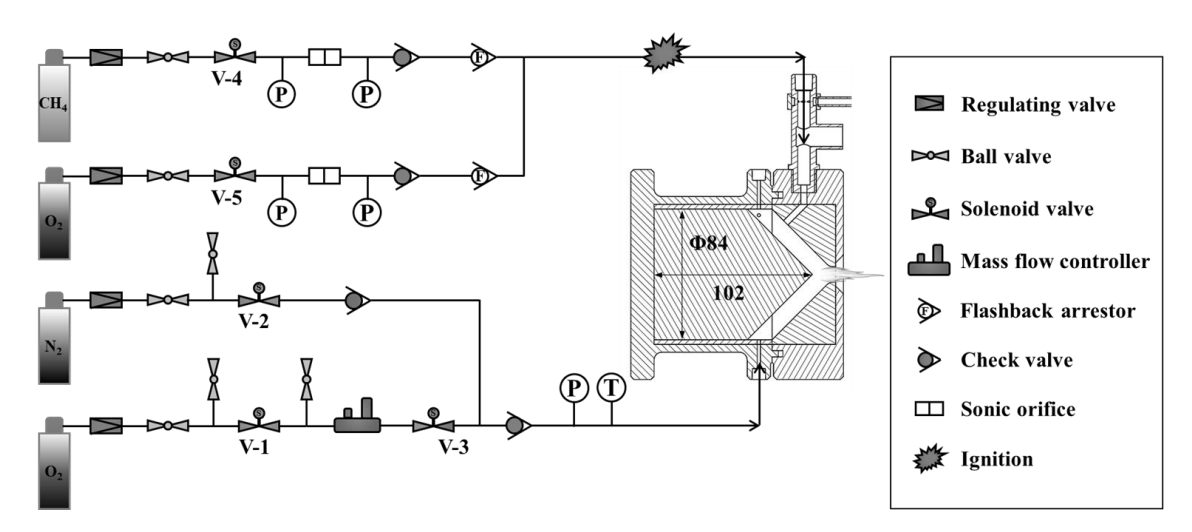


Fig 2. The experimental system for hybrid gas generator

The HGG experimental system established based on the above theoretical analysis is shown in Fig. 2. The system consists of four parts: piping system, ignition system, gas generator, and measurement and control system. The piping system contains four pipelines, respectively used for ignition methane, ignition oxygen, main oxidizer route, and nitrogen supply. The designed structure of the HGG is shown in Fig. 3, with a fuel grain length of 102 mm and a chamber diameter of 84 mm. Swirl injection was used to further enhance the regression rate. Adopting a counterclockwise intake direction, consistent with the rotation direction of the spiral fuel grain used. The nozzle only retained the contraction section to increase combustion chamber pressure, with a throat diameter of 6 mm. The total burning time for firing tests was set to 10s.

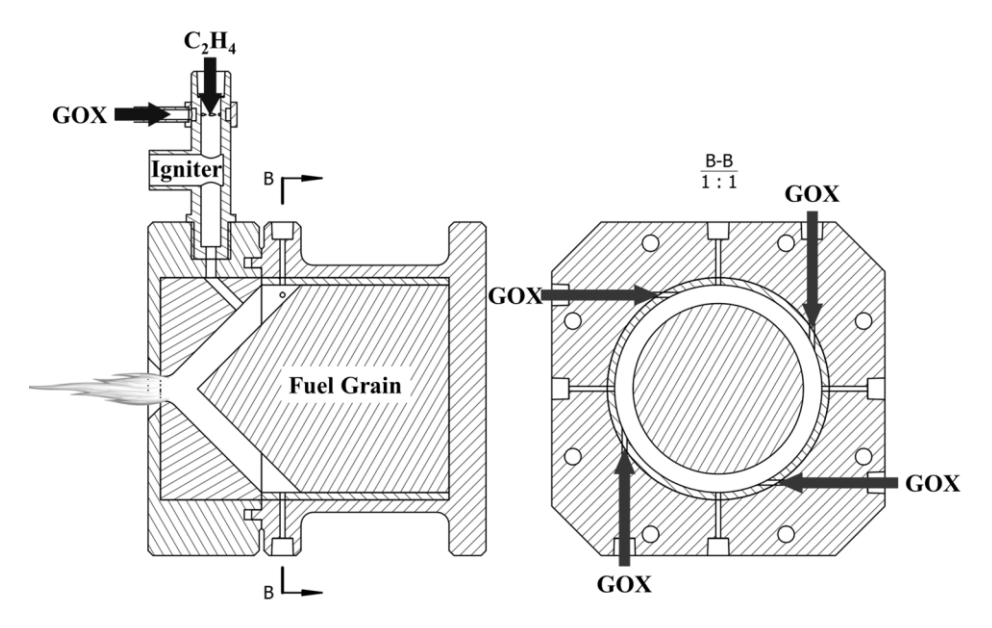


Fig 3. The structure of HGG

#### 3.2. Fuel grains

Seven solid fuel grains from four categories were used in this work with their component shown in Table 1. To further increase the burning surface area and reduce the diameter, a conical structure with the cone angle set at 45° was adopted for the head of the fuel grain.

Type.	Fuel grain	Paraffin	EVA	SA	С	Al	PE	ABS
1	PE	0	0	0	0	0	100%	0
2	P-P	100%	0	0	0	0	0	0
	P-20%Al	80%	0	0	0	20%	0	0
3	P 50%Al	50%	0	0	0	50%	0	0
	P 60%Al	40%	0	0	0	60%	0	0
4	P-B	58%	10%	10%	2%	0	20%	0
7	P-B-ABS	41.76%	7.2%	7.2%	1.44%	0	14.4%	28%

**Table 1.** The composition of fuel grain used in this work

# 4. Experimental setup

# 4.1. Ignition and pressure

Figure 4 shows the variation of combustion chamber pressure for the typical four types of fuel grains. The pressure of all firing tests remained relatively stable. Due to the overall low oxidizer mass flow rate, the adjustment process of the flow controller was not significant from 3.0 s to 7.0 s. After ignition at 7.0 s, a noticeable ignition pressure peak occurred, primarily due to the high supply pressures of

methane and oxygen during the ignition process, which led to a few igniting propellants entering the chamber and participating in combustion. Once this portion of the propellant was consumed, the combustion process tended to stabilize.

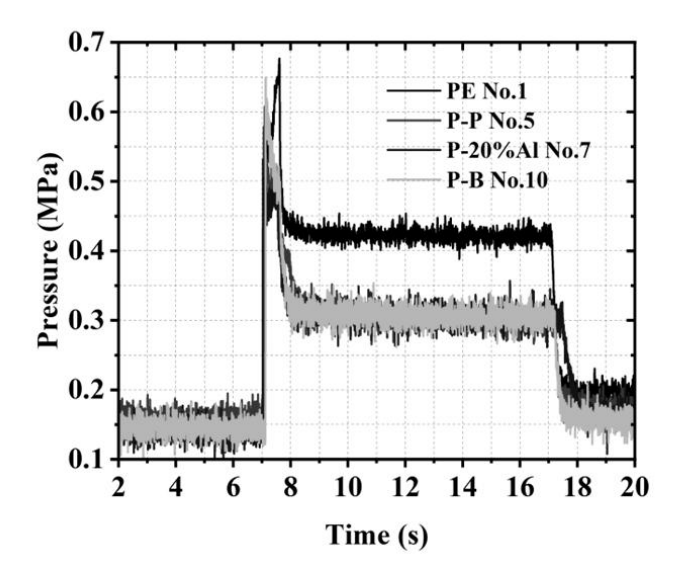


Fig 4. The variation of combustion chamber pressure

### 4.2. Regression rate

The regression rates of PE and P-P propellant grains as a function of oxidizer mass flux are first presented in Fig. 5. Limited by PE's inherent properties, its actual average regression rate is still only 0.267 mm/s even though the oxidizer mass flow rate of 4.87 g/cm²/s is the highest value among all tests. Surprisingly, the regression rates under end-burning configuration were significantly enhanced. With oxidizer mass flux of 0.009-0.0.063 g/cm²·s, the regression rate range of the P-P fuel grain was between 0.55-1.75 mm/s.

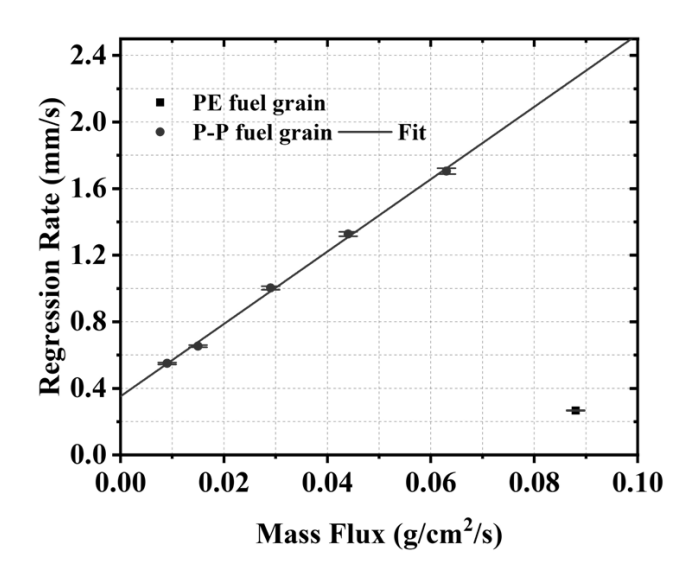


Fig 5. The regression rate of PE and P-P fuel grain

Figure 6 shows these regression rates of different fuel grains with essentially the same oxidizer flux. The regression rate of the P-20%Al fuel grain decreased by 29.5%. As the mass fraction of aluminium powder continued to increase, the regression rate showed a rapid decrease. The regression rate of the P-B fuel grain was significantly lower than that of the P-P fuel grain with a reduction of up to 53.8%.

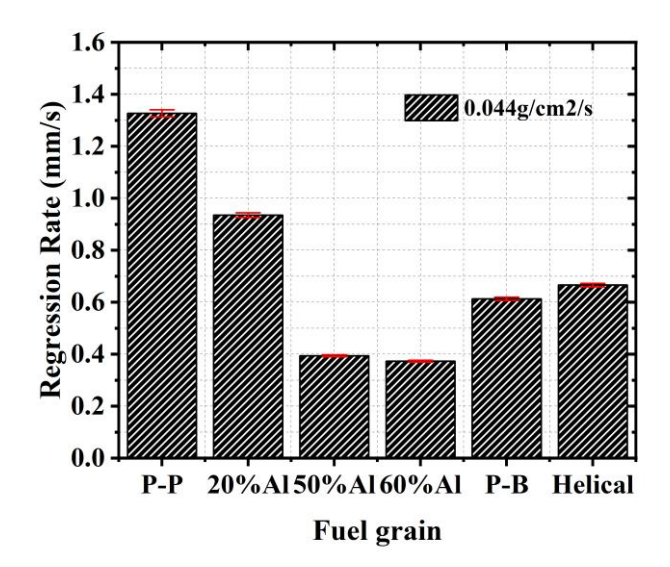
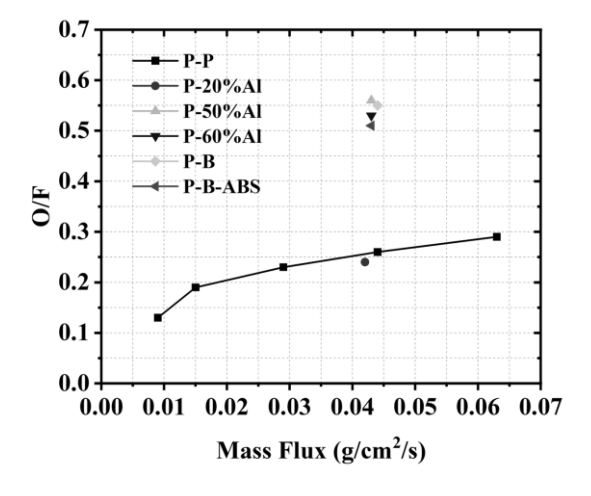


Fig 6. The regression rate of fuel grain with different components and structures

# 4.3. O/F ratio

Figure 7 shows the variation of the average O/F ratio with the oxidizer flux. For the HGG with the regression rate maintaining a linear relationship with the oxidizer flow rate, the observed trend implies that the regression rate was not only controlled by the oxidizer flux but also influenced by the swirl intensity inside the chamber. Higher oxidizer mass flow rate results in a greater swirl intensity in the combustion chamber, leading to an increase in the O/F ratio. In addition, except for the P-20%Al fuel grain, the O/F ratio of the others show a significant increase compared to that of the P-P fuel grain. The addition of a small amount of aluminum powder can increase oxygen consumption, thereby lowering the O/F ratio. However, excessive aluminum powder or other binder components, such as EVA or SA, can lead to a substantial decrease in the regression rate, which then results in an increase in the O/F ratio. This result is consistent with the regression rate data.



**Fig 7.** The variation of O/F ratio with the oxidizer mass flux

#### 5. Conclusion

The combustion characteristics of the paraffin-based HGG were investigated. With a regression rate approaching 2 mm/s, an O/F ratio less than 0.3, and a combustion temperature below 1200 K, paraffin-based HGG represents a high-performance candidate for gas supply. Meanwhile, the addition of aluminum powder and binder significantly decreased the regression rate. Although the high oxygen consumption of aluminum powder resulted in a low O/F ratio at low mass fractions, it increased the

demand for thermal insulation in HGG.

# **Acknowledgements**

This work was funded in part by the National Natural Science Foundation of China (No.12402395, No.92271117), National Key Laboratory of Solid Rocket Propulsion (No. 2024030304), Beijing Key Lab of High Efficiency Space Propulsion Technology and Advanced Space Propulsion Laboratory of BICE (No. LabASP-2024-07), and the Strategic Priority Research Program of the Chinese Academy of Sciences (No. XDB0620202).

#### References

- 1. Tong, X., Cai, G., Zheng, Y., Fang, J.: Optimization of system parameters for gas-generator engines. Acta Astronautica. 59(1-5), 246-252 (2006).
- 2. Hashim, S., Karmakar, S., Roy, A.: Effects of Ti and Mg particles on combustion characteristics of boron–HTPB-based solid fuels for hybrid gas generator in ducted rocket applications. Acta Astronautica. 160, 125-137 (2019).
- 3. Komornik, D., Gany A.: Investigation of a ducted rocket with a paraffin/oxygen hybrid gas generator. Journal of Propulsion and Power. 35(6), 1108-1115 (2019).
- 4. Wang, Z., Lin, X., Li, F., Yu, X.: Combustion performance of a novel hybrid rocket fuel grain with a nested helical structure. Aerospace Science and Technology. 97, (2020).
- 5. Wang, Z., Lin, X., Pan, J., Luo, J., Wang, R., Zhang, Z., Yu, X.: Superior Al90Mg10-based composite fuel grain for a hybrid rocket engine. Journal of Spacecraft and Rockets.: p. 1-9. (2024)
- 6. Wang, Y., Hu, S., Liu, X., Liu, L.: Regression rate modeling of HTPB/paraffin fuels in hybrid rocket motor. Aerospace Science and Technology, 121, (2022).
- 7. Gallo, G., Savino, R.: Regression rate model assessed by ballistic reconstruction technique in hybrid rocket engines burning liquefying fuels. Aerospace Science and Technology, 127, (2022).
- 8. Ozawa, K., Shimada, T.: Effects of O/F shifts on flight performances of vertically launched hybrid sounding rockets. 53rd AIAA/SAE/ASEE Joint Propulsion Conference. AIAA 2017-5051, (2017).
- 9. Migliorino, M., Fabiani, M., Paravan, C., Bianchi, D., Nasuti, F., Galfetti, L., Pellegrini, R., Cavallini, E.: Numerical and experimental analysis of fuel regression rate in a lab-scale hybrid rocket engine with swirl injection. Aerospace Science and Technology. 140, (2023).
- 10. Mazzetti, A., Merotto, L., Pinarello, G.: Paraffin-based hybrid rocket engines applications: A review and a market perspective. Acta Astronautica. 126, 286-297, (2016).
- 11. Zhang, Z., Lin, X., Wang, Z., Wu, K., Luo, J., Fang, S., Zhang, C., Li, F., Yu, X.: Effects of swirl injection on the combustion of a novel composite hybrid rocket fuel grain. Acta Astronautica. 199, 174-182, (2022).
- 12. Sakurai, T., Yuasa, S., Ando, H., Kitagawa, K., Shimada, T.: Performance and regression rate characteristics of 5-kn swirling-oxidizer-flow-type hybrid rocket engine. Journal of Propulsion and Power. 33(4), 891-901, (2017).
- 13. Luo, J., Zhang, Z., Lin, X., Wang, Z., Wu, K., Zhou, G., Zhang, S., Li, F., Yu, X., Wu, J.: Flame dynamics in the combustion chamber of hybrid rocket using multiangle chemiluminescence. Journal of Propulsion and Power. 39(4), 482-491, (2023).